

# Nature of the Magnetic Order in the Charge-Ordered Cuprate $\text{La}_{1.48}\text{Nd}_{0.4}\text{Sr}_{0.12}\text{CuO}_4$

N. B. Christensen,<sup>1,2</sup> H. M. Rønnow,<sup>3,1</sup> J. Mesot,<sup>1</sup> R. A. Ewings,<sup>4</sup> N. Momono,<sup>5</sup>  
M. Oda,<sup>5</sup> M. Ido,<sup>5</sup> M. Enderle,<sup>6</sup> D. F. McMorrow,<sup>7,8</sup> and A. T. Boothroyd<sup>4</sup>

<sup>1</sup> *Laboratory for Neutron Scattering, ETH Zurich & Paul Scherrer Institute, CH-5232 Villigen PSI, Switzerland*

<sup>2</sup> *Materials Research Department, Risø National Laboratory,  
Technical University of Denmark, DK-4000 Roskilde, Denmark*

<sup>3</sup> *Laboratory for Quantum Magnetism, École Polytechnique Fédérale de Lausanne (EPFL), 1015 Lausanne, Switzerland*

<sup>4</sup> *Department of Physics, Oxford University, Oxford, OX1 3PU, United Kingdom*

<sup>5</sup> *Department of Physics, Hokkaido University, Sapporo 060-0810, Japan*

<sup>6</sup> *Institut Laue-Langevin, BP 156 - 38042 Grenoble Cedex 9 - France*

<sup>7</sup> *London Centre for Nanotechnology and Department of Physics and Astronomy, University College London, UK*

<sup>8</sup> *ISIS Facility, Rutherford Appleton Laboratory, Chilton, Didcot, UK*

Using polarized neutron scattering we establish that the magnetic order in  $\text{La}_{1.48}\text{Nd}_{0.4}\text{Sr}_{0.12}\text{CuO}_4$  is either (i) one dimensionally modulated and collinear, consistent with the stripe model or (ii) two dimensionally modulated with a novel noncollinear structure. The measurements rule out a number of alternative models characterized by 2D electronic order or 1D helical spin order. The low-energy spin excitations are found to be primarily transversely polarized relative to the stripe ordered state, consistent with conventional spin waves.

PACS numbers: 74.72.Dn, 75.30.Fv, 75.50.Ee, 75.70.Kw

One of the most striking and robust features in the phenomenology of hole-doped copper oxide superconductors is the four-fold incommensurate (IC) pattern of magnetic neutron scattering peaks centered on the antiferromagnetic (AFM) wave vector of the square  $\text{CuO}_2$  lattice. This pattern is found in the magnetic excitation spectrum of  $\text{YBa}_2\text{Cu}_3\text{O}_{6+y}$  and  $\text{La}_{2-x}(\text{Sr,Ba})_x\text{CuO}_4$  over wide doping ranges [1]. Near  $x = 1/8$  certain La-based materials develop an elastic IC magnetic component accompanied by second order harmonics around the structural Bragg peaks [2, 3, 4]. One school of thought associates these features with one-dimensional (1D) charge modulations separating AFM antiphase bands on the  $\text{CuO}_2$  layers [5]. In this ‘stripe’ model the four-fold pattern is a superposition of two two-fold patterns, arising from spatially separated stripe domains, each with charge modulations along one of the two Cu–O bond directions. Static stripes, posited to occur near  $x = 1/8$ , are thought to compete with superconductivity [6], but dynamic stripes could play a role in the formation of the superconducting state [7].

Recently, however, the stripe picture has been called into question. Several new experimental findings point to the existence of 2D charge density wave order in the ground state of hole-doped cuprates [8, 9]. In addition, the dimensionality of the spin excitation spectrum is a subject of debate [10]. Furthermore, an increasing number of phases exhibiting novel 2D electronic order have been explored theoretically [11], including orbital current correlations [12], checkerboard-type orderings of Cooper pairs [13], and 2D diagonal stripes [14]. The possibility that features previously attributed to stripes might be signatures of a more elaborate 2D ordering makes it vital to obtain information with techniques that can separate

different spatial arrangements of spin and charge.

Here we report a study of the magnetic order and dynamics in  $\text{La}_{1.6-x}\text{Nd}_{0.4}\text{Sr}_x\text{CuO}_4$  (LNSCO;  $x = 0.12$ ) by polarized-neutron scattering. Substitution of Nd for La stabilizes a low-temperature tetragonal structure, which permits the formation, below  $\sim 50$  K, of a robust spin-charge-ordered phase with suppressed superconducting transition temperature  $T_c$ . The relatively large ordered Cu moment  $\sim 0.10\mu_B$  [3] allows detailed neutron polarisation analysis. Below  $T_{\text{Nd}} \simeq 3$  K, Nd–Cu coupling causes alignment of the Nd spins along the  $c$  axis with the same ordering vectors as the Cu spins [3]. At tem-

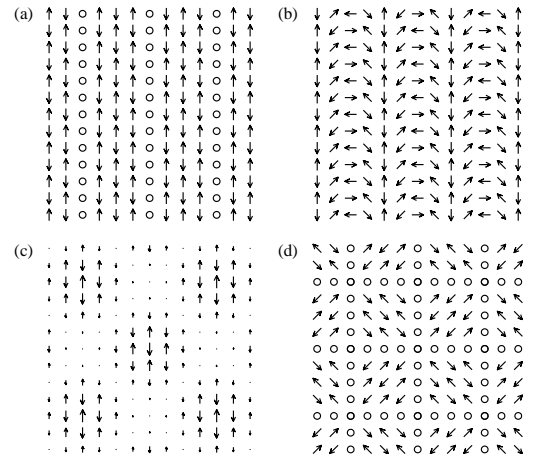


FIG. 1: Models for the magnetic order in La-based cuprates at  $x = 1/8$  doping. (a) One- $\mathbf{q}$  domain with charge stripes (lines of open circles) and collinear spin order [2]. (b) One- $\mathbf{q}$  domain with helical spin order. (c) Collinear two- $\mathbf{q}$  structure of a diagonally modulated commensurate AFM [14]. (d) Two- $\mathbf{q}$  order of charge and spins in a noncollinear structure.

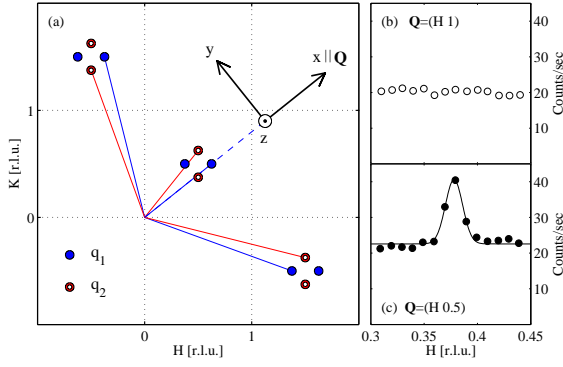


FIG. 2: (a) Reciprocal space of the square  $\text{CuO}_2$  lattice showing the three quartets of magnetic peaks investigated. The peaks are displaced from AFM wave vectors by  $\pm\mathbf{q}_1 = (\pm\delta, 0)$  and  $\pm\mathbf{q}_2 = (0, \pm\delta)$  with  $\delta \simeq x = 0.12$ . Also shown are the axes to which the polarisation  $\mathbf{P}$  and magnetic scattering are referred. (b)-(c) Unpolarized elastic scans through the expected Bragg peak positions for a  $\pi$ -spiral [19].

peratures well above  $T_{\text{Nd}}$  the Nd order is unlikely to influence the ordering pattern and in-plane direction of the Cu spins. We therefore believe that our study of static and dynamic properties of LNSCO at 10 K has direct relevance to the magnetic behaviour of Nd-free higher temperature superconductors. Our results are most naturally understood in terms of a 1D modulation of the AFM order, consistent with the occurrence of stripes, although an exotic 2D noncollinear order is also possible.

Fig. 1 shows four models yielding magnetic diffraction patterns with principal Fourier components  $\mathbf{Q} = (1/2, 1/2) \pm \mathbf{q}_1$  and  $(1/2, 1/2) \pm \mathbf{q}_2$  and equivalent wave vectors, as found experimentally (Fig. 2). Figure 1(a) represents the conventional view [2] that the quartet is due to incoherent superposition of scattering from two equally populated domains with collinear one- $\mathbf{q}$  spin order and orthogonal propagation vectors. From the peak positions alone, this model is indistinguishable from a model of two domains, each with helical one- $\mathbf{q}$  order [15] as sketched in Fig. 1(b). The correct four-fold diffraction pattern is also produced by the collinear two- $\mathbf{q}$  “diagonal stripe” picture [14] in Fig. 1(c) and by the noncollinear two- $\mathbf{q}$  checkerboard structure shown in Fig. 1(d).

Our experiment was performed on the IN20 triple-axis spectrometer at the ILL operated in Heusler-Heusler configuration with a pyrolytic graphite filter to suppress higher order contamination of the scattered beam. The crystal ( $T_c = 6.8$  K), grown by the floating-zone method, contained two grains separated by  $\sim 1^\circ$ . The sample was mounted with the [001] axis vertical in a He cryostat. A final neutron energy of 34.8 meV allowed access to IC quartets surrounding several equivalent AFM wave vectors in the  $(H, K, 0)$  reciprocal lattice plane, denoted  $(H, K)$  for short. The polarisation vector  $\mathbf{P}$  of the neutron beam at the sample position was oriented along

the  $x$ ,  $y$  and  $z$  directions (see below and Fig. 2). The scattered neutrons were recorded in spin-flip (SF) and non-spin-flip (NSF) channels, according to whether their spins had flipped or not on scattering. Corrections for the measured beam polarisation  $P = 0.86 > T_c > T_{\text{Nd}}$ , but some data taken at 1.7 K were used to fix the Bragg peak line shapes from the Nd magnetic order.

The cross section for scattering of polarized neutrons consists of a purely nuclear term, a purely magnetic term and a nuclear-magnetic interference term [16]. We assume that the latter can be neglected at the IC wave vectors of interest, and that the nuclear spins are unpolarized. The magnetic term contains two features that make it possible to determine electronic spin directions. First, magnetic scattering originates only from electronic spin components  $\mathbf{S}_\perp$  perpendicular to  $\mathbf{Q}$ . Second, SF scattering is caused by spin correlations perpendicular to  $\mathbf{P}$  [16]. We denote coherent nuclear scattering by  $N$  and magnetic scattering by  $M_x$ ,  $M_y$  and  $M_z$ , where  $M_\alpha$  is proportional to the time Fourier transform of the correlation function  $\langle S_\alpha(-\mathbf{Q}, 0) S_\alpha(\mathbf{Q}, t) \rangle$  [17]. We define axes such that  $x$  is parallel to  $\mathbf{Q}$ , and  $y$  and  $z$  are perpendicular to  $\mathbf{Q}$  in and out of the scattering plane, respectively, (Fig. 2). With these axes,  $M_x$  is identically zero, and in the absence of a single-domain chiral structure [18] the intensities in the SF and NSF channels with  $\mathbf{P}$  parallel to  $x$ ,  $y$  and  $z$  can be written  $I_{\text{SF}}^x = M_y + M_z + B_{\text{SF}}$ ,  $I_{\text{SF}}^y = M_z + B_{\text{SF}}$ ,  $I_{\text{SF}}^z = M_y + B_{\text{SF}}$ ,  $I_{\text{NSF}}^x = N + B_{\text{NSF}}$ ,  $I_{\text{NSF}}^y = N + M_y + B_{\text{NSF}}$  and  $I_{\text{NSF}}^z = N + M_z + B_{\text{NSF}}$ , where  $B_{\text{SF}}$  and  $B_{\text{NSF}}$  are the backgrounds. These expressions apply both to elastic ( $t = \infty$ ) and inelastic scattering.

We first treat elastic scattering, in which case  $M_y$ ,  $M_z$  are proportional to the squares of the corresponding ordered spin components. At each of the three IC quartets indicated in Fig. 2 the neutron count rate was recorded in some or all six polarisation channels at each temperature. The purpose of probing several zones is to vary the orientation of  $\mathbf{Q}$  relative to the ordered spin direction so that the magnetic cross sections  $M_y$  and  $M_z$  change.

Fig. 3 shows data obtained by scanning the sample rotation angle  $\theta$  through the  $(1/2, 1/2) + \mathbf{q}_1$  satellite peak with  $\mathbf{P} \parallel z$ . The SF and NSF channels then sense  $M_y$  and  $M_z$ , respectively. The strong NSF signal at 1.7 K [Fig. 3(a)] implies significant elastic scattering from magnetic moments oriented perpendicular to the  $\text{CuO}_2$  planes. On heating to 10 K the NSF signal almost vanishes [Fig. 3(b)]. A weak signal is present in the SF channel at both 1.7 K and 10 K [Figs. 3(c) and (d)]. These observations directly confirm an earlier finding that the Nd moments order along the  $c$  axis [3]. Analysis of the data in Figs. 3(b) and (d) indicates that at 10 K the spin direction is mainly confined to the  $\text{CuO}_2$  planes. The data do not rule out a small ordered component along  $c$ , but as the presence or absence of such a component does not alter our conclusions, which refer to the in-plane order, we

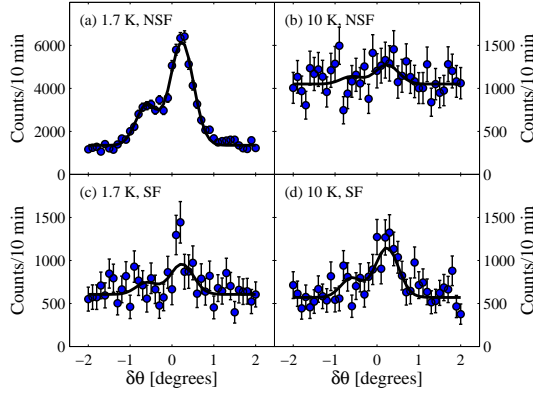


FIG. 3: SF and NSF elastic scattering at  $(1/2, 1/2) + \mathbf{q}_1$  with  $\mathbf{P} \parallel z$ . The two-peak line shape is due to the presence of two crystallites separated by  $\sim 1^\circ$ . The solid line in (a) is a fit to two Gaussians. The lines in (b)–(d) were obtained from a fit to the same line shape as in (a) but with the overall intensity scale and background allowed to vary.

assume that at 10 K the Cu spins lie in the  $\text{CuO}_2$  planes.

We now turn to the spatial arrangement and in-plane orientation of the Cu moments. Figure 4 shows  $M_y$  at three IC peaks of type  $\mathbf{q}_1$  and at three peaks of type  $\mathbf{q}_2$ . The  $\mathbf{q}_1$  and  $\mathbf{q}_2$  peaks close to  $(1/2, 1/2)$  have roughly equal intensity. By contrast, near  $(-1/2, 3/2)$  the  $\mathbf{q}_1$  peak is clearly weaker than the  $\mathbf{q}_2$  peak, while the situation is reversed near  $(3/2, -1/2)$ .

The relative intensities of the peaks in any given quartet depend on (i) the orientation of  $\mathbf{Q}$  relative to the spin components contributing to the peaks and (ii) the population of any equivalent magnetic domains. For the one- $\mathbf{q}$  order in Fig. 1(b), the  $\mathbf{q}_1$  satellites around  $(-1/2, 3/2)$  should have same intensity as those around  $(3/2, -1/2)$ , in disagreement with the data. This is true also for more than one chiral domain [16], because all in-plane spin directions contribute equally to each peak. Considering next the collinear, two- $\mathbf{q}$  model in Fig. 1(c), the angle between  $\mathbf{Q}$  and the unique spin direction of a single domain changes only slightly between  $\mathbf{q}_1$  and  $\mathbf{q}_2$  in any given quartet, so the large intensity differences observed in  $M_y$  near  $(-1/2, 3/2)$  and  $(3/2, -1/2)$  cannot be reproduced by this model. Hence, we can rule out both in-plane helical order [Fig. 1(b)] and “diagonal stripes” [Fig. 1(c)], as well as the so-called  $\pi$ -spiral model [19] because that produces  $\mathbf{q}_j$  satellites about  $(1/2, 1)$ -type positions which are not observed, as shown in Fig. 2(b) and 2(c).

By contrast, the data are consistent with two, equally populated, one- $\mathbf{q}$  domains, each with collinear spin order, and spins  $\langle \mathbf{S} \rangle_j$  of domain  $j$  approximately perpendicular to  $\mathbf{q}_j$  as shown for one domain in Fig. 1(a). In this scenario, the  $\mathbf{q}_1$  and  $\mathbf{q}_2$  peaks near  $(1/2, 1/2)$  have nearly identical intensities because the angle between  $\mathbf{Q}$  and  $\langle \mathbf{S} \rangle_j$  is the same for both domains. Conversely, near

$(-1/2, 3/2)$ , the  $\mathbf{q}_1$  ( $\mathbf{q}_2$ ) peak is relatively weak (strong) since the corresponding spins are close to being parallel (perpendicular) to  $\mathbf{Q}$ . Around  $(3/2, -1/2)$  these angular factors switch, and the  $\mathbf{q}_1$  peak should be the most intense, as observed. The solid lines in Fig. 4 are calculations based on this model. As in Fig. 3, the line shape at each  $\mathbf{Q}$  was fixed by fitting the large Nd signal in  $I_{\text{NSF}}^z$  at 1.7 K. The corresponding curves were then multiplied by the modulation expected for in-plane spins  $\langle \mathbf{S} \rangle_j$  perpendicular to  $\mathbf{q}_j$  and corrected for the form factor difference between the Nd-dominated 1.7 K signal and the 10 K Cu signal. Although the calculations do not agree in every detail, they clearly reproduce the salient features of the data. Quantitatively, a least-squares fit to all the data in Fig. 4 results in  $\langle \mathbf{S} \rangle_1 \perp \mathbf{q}_1$  and  $\langle \mathbf{S} \rangle_2 \perp \mathbf{q}_2$  with a  $\pm 3^\circ$  accuracy. Our diffraction data are thus consistent with an *incoherent* superposition of orthogonal stripe domains.

Our data are also consistent with the two- $\mathbf{q}$  structure shown in Fig. 1(d), which is a *coherent* superposition of two orthogonal stripe domains and produces the correct observed positions for both charge and magnetic peaks. This has two implications. First, one cannot infer the existence of 1D stripes from existing measurements of charge and magnetic peak positions [2, 5], and second, although our results do not rigorously rule out a checkerboard configuration, they do impose the noncollinear spin arrangement shown in Fig. 1(d) on any such model.

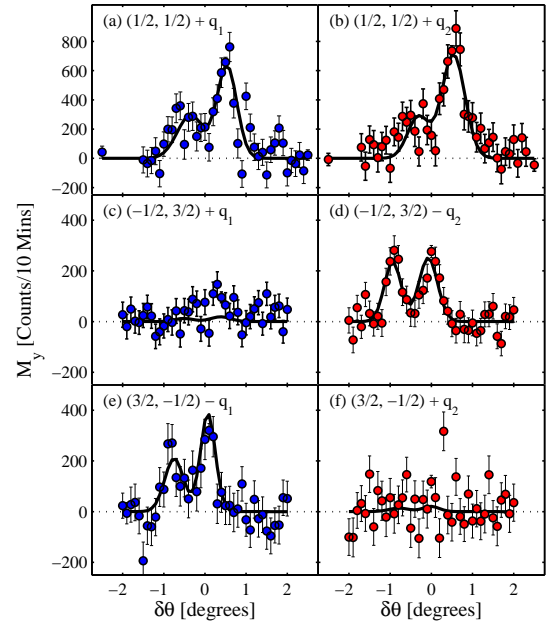


FIG. 4: Processed polarized-neutron data taken at  $T = 10$  K, showing the in-plane component  $M_y$  of the magnetic cross section at each of six IC peaks of type  $\mathbf{q}_1$  (left) and  $\mathbf{q}_2$  (right).  $M_y$  was calculated both from the SF data ( $M_y = I_{\text{SF}}^x - I_{\text{SF}}^y$ ) and from the NSF data ( $M_y = I_{\text{NSF}}^y - I_{\text{NSF}}^x$ ). After checking for consistency, data thus obtained were combined. The solid lines represent the model calculation described in the text.

Wavevector $\mathbf{Q}$	Cross-section component	Intensity
$(-1/2, 3/2) + \mathbf{q}_1$	$M_y$	$7.4 \pm 1.3$
$(-1/2, 3/2) + \mathbf{q}_1$	$M_z$	$9.9 \pm 1.4$
$(3/2, -1/2) - \mathbf{q}_1$	$M_y$	$2.4 \pm 1.1$
$(3/2, -1/2) - \mathbf{q}_1$	$M_z$	$7.6 \pm 1.1$
Excitation components relative to [010]		
Transverse, out-of-plane		$8.8 \pm 0.9$
Transverse, in-plane		$7.8 \pm 1.4$
Longitudinal, in-plane		$1.7 \pm 1.3$

TABLE I: Processed inelastic ( $\hbar\omega = 5$  meV) count rates per 10 minutes at  $T = 10$  K.  $M_y$  and  $M_z$  were obtained from  $I_{\text{SF}}^x - I_{\text{SF}}^y$  and  $I_{\text{SF}}^x - I_{\text{SF}}^z$ , respectively. Total time: 44 h.

For inelastic scattering,  $M_z$  is sensitive to spin fluctuations out of the scattering plane and  $M_y$  to in-plane fluctuations perpendicular to  $\mathbf{Q}$ . Table I shows the count rates at  $(-1/2, 3/2) + \mathbf{q}_1$  and  $(3/2, -1/2) - \mathbf{q}_1$  at  $\hbar\omega = 5$  meV. There is a statistically significant difference between the values of  $M_y$  at the two wave vectors. This shows that the low-energy spin fluctuations in LNSCO have a preferred direction, and it implies that they are not of the singlet-triplet type (for which we would expect  $M_y = M_z$ ). The data are naturally explained by the  $\mathbf{q}_1$  stripe domain shown in Fig. 1(a). Converting from  $M_y$  to components transverse to and along  $\langle \mathbf{S} \rangle_1$  shows (Table I) that the fluctuations are predominantly transverse, consistent with spin waves. This finding supports theories of the cuprate spin excitation spectrum based on a ground state with slowly fluctuating stripelike correlations, in which the low-energy excitations resemble Goldstone modes of weakly coupled spin ladders [20].

In summary, we have shown that the magnetic order in the spin-charge ordered cuprate  $\text{La}_{1.48}\text{Nd}_{0.4}\text{Sr}_{0.12}\text{CuO}_4$  is either modulated in 1D only (with spins perpendicular to the modulation direction) or takes the form of a previously unconsidered noncollinear two- $\mathbf{q}$  structure. In the former case, it is reasonable to conclude that charge order is also one-dimensional, consistent with a stripe model.

We thank J.P. Hill, J.M. Tranquada and S.A. Kivelson for stimulating discussions. Support was provided by: Danish Natural Science Council via DanScatt, Danish Technical Research Council Framework Program on Superconductivity (N. B. C.), Wolfson Royal Society (D. F. M.), and EPSRC of Great Britain (R. A. E.).

- Mook *et al.*, Nature **395**, 580 (1998); P. Dai *et al.*, Phys. Rev. B **63**, 054525 (2001).
- [2] J. M. Tranquada *et al.*, Nature **375**, 561 (1995).
- [3] J. M. Tranquada *et al.*, Phys. Rev. B **54**, 7489 (1996).
- [4] M. Fujita *et al.*, Phys. Rev. B **66**, 184503 (2002); **70**, 104517 (2004);
- [5] S. A. Kivelson *et al.*, Rev. Mod. Phys. **75**, 1201 (2003).
- [6] A. R. Moodenbaugh *et al.*, Phys. Rev. B **38**, 4596 (1988); K. Kumagai *et al.*; J. Mag. Mag. Mat. **76–77**, 601 (1988); J. M. Tranquada *et al.*, Phys. Rev. Lett. **78**, 338 (1997).
- [7] V. J. Emery *et al.*, Phys. Rev. B **56**, 6120 (1997); Yu. A. Krotov *et al.*, Phys. Rev. B **56**, 8367 (1997); H. Johansson and G. I. Japaridze, Phys. Rev. B **68**, 214507 (2003).
- [8] J. E. Hoffman *et al.*, Science **295**, 466 (2002); T. Hanaguri *et al.*, Nature **430**, 1001 (2004).
- [9] S. Komiya *et al.*, Phys. Rev. Lett. **94**, 207004 (2005).
- [10] S. M. Hayden *et al.*, Nature **429**, 531 (2004); J. M. Tranquada *et al.*, Nature **429**, 534 (2004); N. B. Christensen *et al.*, Phys. Rev. Lett. **93**, 147002 (2004); V. Hinkov *et al.*, Nature **430**, 650 (2004); P. Bourges *et al.*, Science **288**, 1234 (2000); C. Stock *et al.*, Phys. Rev. B **71**, 024522 (2005).
- [11] S. Sachdev, Science **288**, 475 (2000).
- [12] X. G. Wen and P. A. Lee, Phys. Rev. Lett. **76**, 503 (1996); C. M. Varma, Phys. Rev. B **55**, 14554 (1997); S. Chakravarty *et al.*, Phys. Rev. B **63**, 094503 (2001).
- [13] M. Vojta, Phys. Rev. B **66**, 104505 (2002); H. D. Chen *et al.*, Phys. Rev. Lett. **93**, 187002 (2004); Z. Tesanovic, Phys. Rev. Lett. **93**, 217004 (2004); H. X. Huang *et al.*, Phys. Rev. B **71**, 184514 (2005); P. W. Anderson cond-mat/0406038.
- [14] B. V. Fine, Phys. Rev. B **70**, 224508 (2004).
- [15] B. I. Shraiman and E. D. Siggia, Phys. Rev. Lett. **62**, 1564 (1989); P.-A. Lindgård, Phys. Rev. Lett. **95**, 217001 (2005).
- [16] R. M. Moon *et al.*, Phys. Rev. **181**, 920 (1969)
- [17] G. L. Squires, *Introduction to the theory of thermal neutron scattering*, (Dover, New York, 1996).
- [18] The cross section for a polarized incident beam is proportional to  $\mathbf{S}_\perp(-\mathbf{Q}, \mathbf{0}) \cdot \mathbf{S}_\perp(\mathbf{Q}, \mathbf{t})$  plus a polarisation-dependent chiral term proportional to  $\mathbf{P} \cdot (\mathbf{S}_\perp(-\mathbf{Q}, \mathbf{0}) \times \mathbf{S}_\perp(\mathbf{Q}, \mathbf{t}))$  [16]. A single-domain chiral structure should reveal itself in the total scattering (SF+NSF) as an excess of intensity for  $x$  polarisation relative to  $y$  and  $z$  polarisation. At all wave vectors studied at 10 K, the chiral contribution vanishes within experimental error. On average it amounts to  $1 \pm 5\%$  of the polarisation-independent scattering.
- [19] M.B. Silva Neto, cond-mat/0609539.
- [20] M. Vojta and T. Ulbricht, Phys. Rev. Lett. **93**, 127002 (2004); G. S. Uhrig *et al.*, Phys. Rev. Lett. **93**, 267003 (2004); G. Seibold and J. Lorenzana, Phys. Rev. Lett. **94**, 107006 (2005); B. M. Andersen and P. Hedegård, Phys. Rev. Lett. **95**, 037002 (2005); D. X. Yao, E. W. Carlson and D. K. Campbell, Phys. Rev. Lett. **97**, 017003 (2006).

[1] S-W. Cheong *et al.*, Phys. Rev. Lett. **67**, 1791 (1991); K. Yamada *et al.*, Phys. Rev. B **57**, 6165 (1998); H. A.